Journal of Alloys and Compounds, 197 (1993) 43–49
JALCOM 638

The formation of the $L1_2$ ordered structure in hypostoichiometric Pd_3Mn alloys containing interstitial boron

Y. Sakamoto, K. Takao and Y. Nagaoka
Department of Materials Science and Engineering, Nagasaki University, Nagasaki 852 (Japan)

T. B. Flanagan
Department of Chemistry, The University of Vermont, Burlington, VT 05405-0125 (USA)

(Received December 8, 1992)

Abstract

The ordering of the $L1_2$ structure in hypostoichiometric Pd_3Mn alloys containing interstitial boron, *i.e.* $Pd_{3+x}Mn_{1-x}B_y$ with $x=0.2$ and 0.4 and $y=0.27$ and 0.53, and for comparison in $Pd_{3.2}Mn_{0.8}M_{0.27}$ with substitutional alloying elements M ≡ Ag, Cu and Ni has been studied by X-ray, electron diffraction and electrical resistance measurements. The results clearly indicate the presence of the $L1_2$ (Cu_3Au) type of superlattice in addition to small amounts of regions containing superimposed $L1_{2-s}$ and $L1_2$ superlattices. For alloys of $Pd_{3.4}Mn_{0.6}B_y$ with $y=0.27$ and $Pd_{3.2}Mn_{0.8}M_{0.27}$ with M ≡ Ag, Cu and Ni, however, this was not the case. It is suggested that the formation of the $L1_2$ structure in the alloys at high temperature requires the presence of the $L1_{2-s}$ structure and an interstitial boron content greater than about $y=0.15$. Thus the order transition $L1_{2-s} \rightarrow L1_2$ in $Pd_{3+x}Mn_{1-x}B_y$ is associated with the preferential occupation of boron atoms at particular octahedral sites of the $L1_{2-s}$ structure.

1. Introduction

The present authors [1] have recently observed from X-ray, electron diffraction and electrical resistance measurements that Pd_3MnB_y alloys with about $y=0.125$–0.2 have two types of ordered structures: $L1_{2-s}$ and $L1_2$ (Cu_3Au). The former has a long-period one-dimensional antiphase domain structure with a domain size $M=2$ [2–5] and the electron diffraction patterns of the annealed alloys with these B contents, obtained by slow cooling from about 1153 K, show mainly two-variant $L1_{2-s}$ reflections accompanied by the formation of twinned structures. However, after quenching from high temperatures the $L1_2$ ordered structure is observed, but in some regions of these alloys the electron diffraction patterns exhibit weak and diffuse reflections which are due to the superimposition of both $L1_{2-s}$ and $L1_2$ superlattice.

It has thus been found that in high boron content Pd_3Mn alloys the transition long-range order (LRO) $L1_{2-s} \rightleftarrows L1_2 + (L1_{2-s} + L1_2)$ occurs instead of the transition LRO ⇄ short-range order (SRO) of the $L1_{2-s}$ structure observed previously in boron-free Pd_3Mn alloy [2–5]. The reason for the stability of the $L1_2$ structure at higher temperature in Pd_3Mn alloys with high boron content is unknown, but the formation of the $L1_2$ structure may be initiated at the periodic antiphase domain boundaries of the $L1_{2-s}$ owing to lattice expansion caused by the preferential occupation of boron atoms at octahedral sites consisting of six palladium nearest-neighbour atoms [6].

The purpose of this study is to examine the transition behaviour of the $L1_2$ and $L1_{2-s}$ structures in hypostoichiometric Pd_3Mn alloys containing boron. The important role of boron in structural intermetallic compounds is well known [7] and we wish to extend the study of its role in ordering reactions of Pd_3Mn to the hypostoichiometric alloys in this work. The crystal structures of boron-free hypostoichiometric Pd_3Mn alloys, *e.g.* alloys of $Pd_{3.2}Mn_{0.8}$ (Pd–20.0at.%Mn) and $Pd_{3.4}Mn_{0.6}$ (Pd–15.0at.%Mn), quenched from about 1173 K are almost completely of the α-f.c.c. disordered type, although electron diffraction patterns for the 20 at.% Mn alloy do show faint reflections from $L1_{2-s}$. Both the fully annealed B-free alloys have the short-range-ordered $L1_{2-s}$ structure [8, 9].

2. Experimental details

The alloy samples were prepared as described previously [1]. The compositions used in this study were $Pd_{3.2}Mn_{0.8}B_{0.27}$ (B:Mn atom ratio $r_B=0.0675$), $Pd_{3.2}Mn_{0.8}B_{0.53}$ ($r_B=0.1325$), $Pd_{3.4}Mn_{0.6}B_{0.27}$ ($r_B=$

0925-8388/93/$6.00

0.0675) and $Pd_{3.4}Mn_{0.6}B_{0.53}$ ($r_B = 0.1325$) in addition to the previously examined boron-free alloys $Pd_{3.2}Mn_{0.8}$, *i.e.* Pd–20.0at.%Mn, and $Pd_{3.4}Mn_{0.6}$, *i.e.* Pd–15.0at.%Mn. Furthermore, for comparison $Pd_{3.2}Mn_{0.8}M_{0.27}$ alloys with M ≡ Ag, Cu and Ni were also examined where the alloying elements M formed substitutional alloys.

Before the X-ray, electron diffraction and electrical resistance measurements were performed, the following heat treatments were carried out:

(1) The samples were quenched rapidly into ice-water after heating at about 1173 K for 10 min in a stream of argon gas. The samples will be referred to as "quenched".

(2) The samples were slowly cooled *in vacuo* to room temperature from about 1153 K at a rate of 10 K h^{-1}. These samples will be referred to as "annealed".

The techniques and procedures used for quenching and measurements of the physical properties have been described previously [1, 4, 5, 8, 9].

According to the electrical resistance *vs.* temperature relationship determined previously, in order to examine the behaviour of the ordering transitions, electron diffraction studies were carried out separately using initially quenched samples which were also heated and cooled to the specified temperatures and then quenched into ice-water from the quenching temperatures during the heating and cooling processes.

3. Results and discussion

3.1. X-Ray diffraction studies

The X-ray diffraction patterns of $Pd_{3.2}Mn_{0.8}B_y$ and $Pd_{3.4}Mn_{0.6}B_y$ alloys with $y = 0.27$ and 0.53 are shown in Figs. 1 and 2 respectively. The upper parts of the figures show the patterns of quenched alloys and the lower parts those of annealed alloys. The diffraction patterns reveal only a single α-f.c.c. Pd and the ordered $L1_2$ phases. The open circles in the figures indicate the $L1_2$ reflections. As will be described later, the α-Pd phase corresponds to the short-range-ordered $L1_{2-s}$ structure, where the degree of SRO is greater in the annealed samples of high manganese and low boron content alloys.

It can be seen that the formation of the $L1_2$ phase is more favourable for $Pd_{3.2}Mn_{0.8}B_y$ than for $Pd_{3.4}Mn_{0.6}B_y$ and the formation is easier for high boron content alloys at higher temperatures, because the $L1_2$ reflections are not observed in an annealed sample of $Pd_{3.4}Mn_{0.6}B_y$ with $y = 0.27$. This implies that the formation of the $L1_2$ structure occurs through the $L1_{2-s}$ structure at high temperature, because, as has been observed, the quenched alloy of boron-free $Pd_{3.4}Mn_{0.6}$ (Pd–15.0at.%Mn) is in an almost disordered f.c.c. state, whereas boron-free $Pd_{3.2}Mn_{0.8}$ (Pd–20.0at.%Mn) alloy

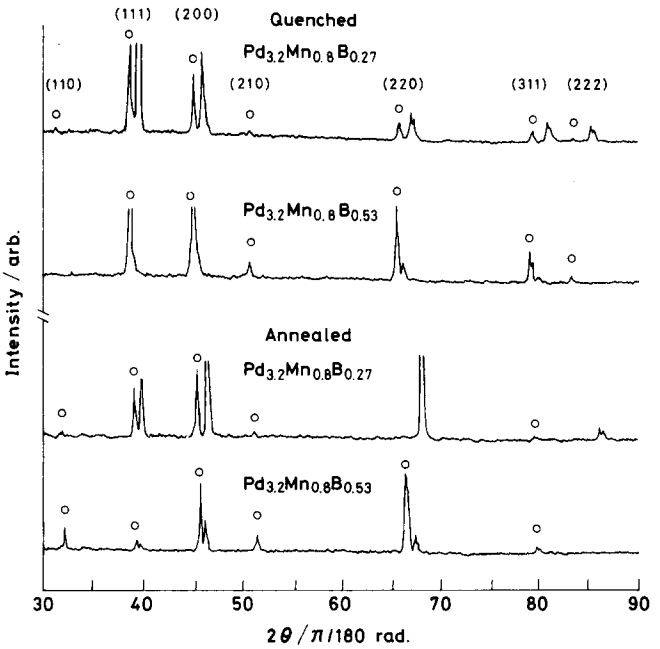

Fig. 1. X-Ray diffraction line profiles of both quenched (upper) and annealed (lower) alloys of $Pd_{3.2}Mn_{0.8}B_y$ with $y = 0.27$ and 0.53 at room temperature. The open circles indicate diffraction lines of the $L1_2$ phase. Cu Kα radiation with a nickel filter was used.

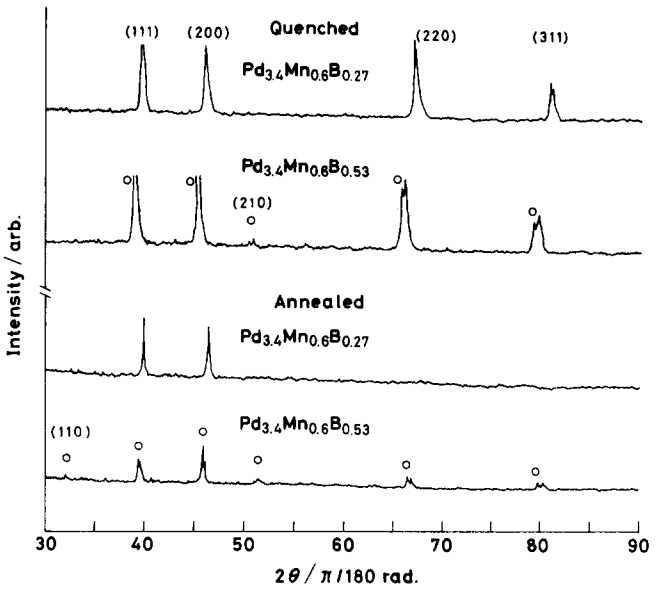

Fig. 2. X-Ray diffraction line profiles of both quenched (upper) and annealed (lower) alloys of $Pd_{3.4}Mn_{0.6}B_y$ with $y = 0.27$ and 0.53 at room temperature. The open circles indicate diffraction lines of the $L1_2$ phase. Cu Kα radiation with a nickel filter was used.

has short-range order of $L1_{2-s}$ at higher temperature quenching. Furthermore, it can be seen that the $L1_2$ structure in hypostoichiometric Pd_3Mn alloys with high boron content is more stabilized compared with that in the previously examined stoichiometric Pd_3Mn [1], because X-ray diffraction due to the $L1_2$ structure is

observed even in annealed alloys obtained by slow cooling.

Figure 3 shows the lattice parameters of the α-Pd and $L1_2$ phases in $Pd_{3.2}Mn_{0.8}B_y$ and $Pd_{3.4}Mn_{0.6}B_y$ alloys as a function of boron content y together with the previously determined lattice parameters of Pd_3MnB_y [1]. The lattice parameters of the α-Pd phase are larger for the as-quenched than for the annealed alloys and at the same high boron contents the lattice parameters increase in the sequence Pd_3MnB_y, $Pd_{3.2}Mn_{0.8}B_y$, $Pd_{3.4}Mn_{0.6}B_y$. The lattice expansion of the α-Pd phase in high boron content $Pd_{3.4}Mn_{0.6}B_y$ alloys is almost the same as that in binary Pd–B solid solution alloys [10–13] when comparing the same unit of B concentration, *i.e.* Pd_4B_y. The lattice parameters of the $L1_2$ phase formed in these B-containing hypostoichiometric alloys are considerably larger than those in Pd_3MnB_y. The larger lattice expansion in the lower manganese content alloys is attributed to the fact that in addition to boron occupation of particular interstices of the short-range-ordered $L1_{2-s}$ structure, it also occupies particular octahedral interstices in the α-f.c.c. disordered phase and the latter causes a larger expansion.

On the other hand, the X-ray diffraction patterns of both quenched and annealed $Pd_{3.2}Mn_{0.8}M_{0.27}$ alloys with M ≡ Ag, Cu and Ni revealed only an α-f.c.c. disordered phase and no $L1_2$ ordered phase. This implies that these elements alloy only substitutionally. The lattice parameters of these alloys decreased in the sequence expected as a result the decreasing atom radii of Ag, Cu and Ni. The derived a_o values for the quenched alloys were (± 0.0002 nm) $a_o = 0.3908$ nm for $Pd_{3.2}Mn_{0.8}Ag_{0.27}$, $a_o = 0.3882$ nm for $Pd_{3.2}Mn_{0.8}Cu_{0.27}$ and $a_o = 0.3879$ nm for $Pd_{3.2}Mn_{0.8}Ni_{0.27}$. The values for the annealed samples were $a_o = 0.3902$ nm for $Pd_{3.2}Mn_{0.8}Ag_{0.27}$, $a_o = 0.3879$ nm for $Pd_{3.2}Mn_{0.8}Cu_{0.27}$ and $a_o = 0.3877$ for $Pd_{3.2}Mn_{0.8}Ni_{0.27}$.

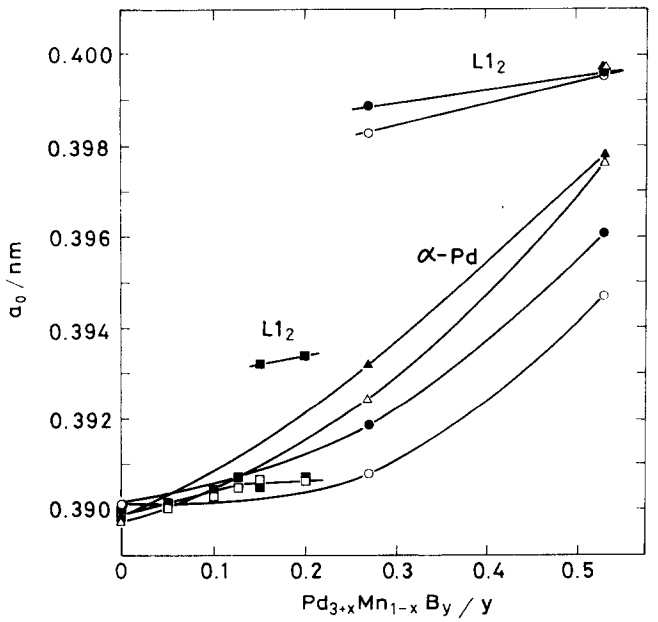

Fig. 3. Room temperature lattice parameters of α-Pd and $L1_2$ phases in $Pd_{3+x}Mn_{1-x}B_y$ alloys as a function of boron content y together with previously determined lattice parameters of Pd_3MnB_y [1]. $Pd_{3.2}Mn_{0.8}B_y$: ●, quenched; ○, annealed. $Pd_{3.4}Mn_{0.6}B_y$: ▲, quenched; △, annealed. Pd_3MnB_y: ■, quenched; □, annealed.

3.2. *Electron microscopy and electrical resistance measurements*

The electron diffraction patterns with [001] incidence for both quenched and annealed alloys of $Pd_{3.2}Mn_{0.8}B_y$ with $y = 0.27$ and $Pd_{3.4}Mn_{0.6}B_y$ with $y = 0.27$ and 0.53 are shown in Figs. 4 and 5 respectively. It was found that in the quenched samples of all the alloys except for $Pd_{3.4}Mn_{0.6}B_y$ with $y = 0.27$ (Fig. 5(a)) some regions exhibit strong reflections due to the $L1_2$ structure (Figs. 4(a) and 5(c)) and others show relatively weak and diffuse reflections which are considered to be a superimposition of the $L1_2$ and $L1_{2-s}$ superlattices (Figs. 4(b) and 5(d)). However, in both quenched and annealed alloys of $Pd_{3.4}Mn_{0.6}B_y$ with $y = 0.27$ strong $L1_2$ reflections are not observed (Figs. 5(a) and 5(b)); this is due to a small amount of the $L1_{2-s}$ structure and consequently only a small amount of boron in the $L1_{2-s}$ alloy. In contrast, the diffraction patterns for a quenched $Pd_{3.2}Mn_{0.8}B_y$ alloy with $y = 0.53$ (not given here) showed almost only strong $L1_2$ reflections throughout the sample.

On the other hand, for the annealed samples of all the alloys except for $Pd_{3.4}Mn_{0.6}B_y$ with $y = 0.27$ (Fig. 5(b)), in addition to the strong reflections of $L1_2$ in some regions (Figs. 4(c) and 5(e)), others show also relatively weak and diffuse superimposed reflections of $L1_2$ and $L1_{2-s}$; however, for the annealed sample of

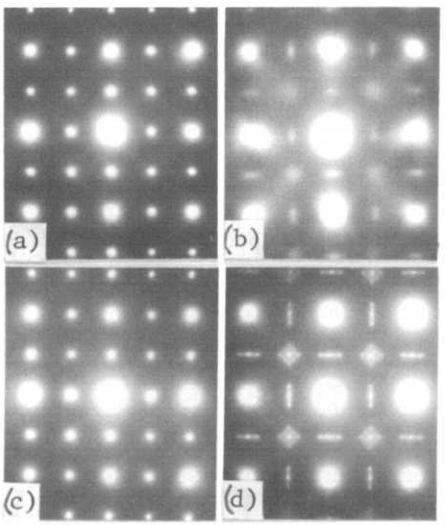

Fig. 4. Electron diffraction patterns with [001] incidence for as-quenched (a), (b) and annealed (c), (d) alloys of $Pd_{3.2}Mn_{0.8}B_y$ with $y = 0.27$.

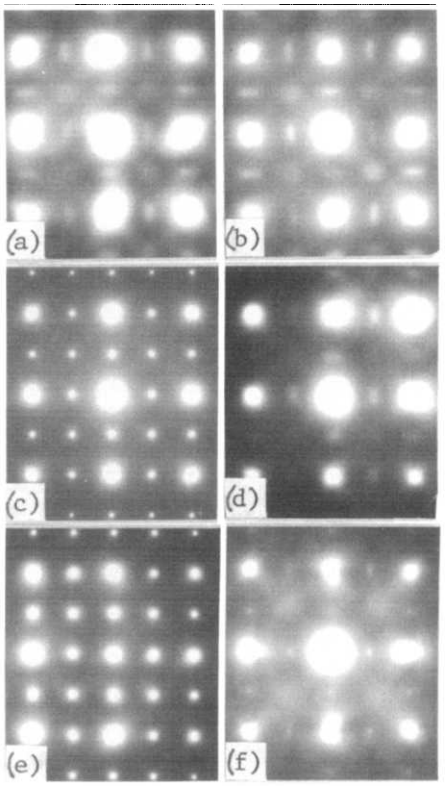

Fig. 5. Electron diffraction patterns with [001] incidence for as-quenched (a), annealed (b) alloys of $Pd_{3.4}Mn_{0.6}B_y$ with $y=0.27$ and also for as-quenched (c), (d) and annealed (e), (f) alloys of $Pd_{3.4}Mn_{0.6}B_y$ with $y=0.53$.

$Pd_{3.2}Mn_{0.8}B_y$ with $y=0.53$ relatively clear but weak reflections due to only $L1_{2-s}$ were mainly observed (Fig. 4(d)), and for the annealed sample of $Pd_{3.4}Mn_{0.6}B_y$ with $y=0.53$ faint reflections due to $L1_2$ were observed (Fig. 5(f)). In the annealed samples of these hypo-stoichiometric Pd_3Mn alloys containing boron the formation of the twinned structures was not observed, although in the annealed samples of the stoichiometric Pd_3Mn alloys with high B content many twinned structures have been introduced, together with the appearance of strong two-variant reflections of $L1_{2-s}$ [1]. These results of electron diffraction studies are in agreement with those of X-ray diffraction studies mentioned above.

Figures 6 and 7 show electrical resistance *vs.* temperature relationships for $Pd_{3.2}Mn_{0.8}B_y$ and $Pd_{3.4}Mn_{0.6}B_y$ alloys respectively together with the previously determined electrical resistance behaviour of boron-free alloys of $Pd_{3.2}Mn_{0.8}$ (Pd–20.0at.%Mn) and $Pd_{3.4}Mn_{0.6}$ (Pd–15.0at.%Mn) [5, 9] for comparison. The arrows with letter labels in the figures indicate temperatures from which samples were quenched into ice-water and then examined by electron diffraction. The results of electron diffraction and transmission electron microscopy observations for these alloys are summarized in Table 1.

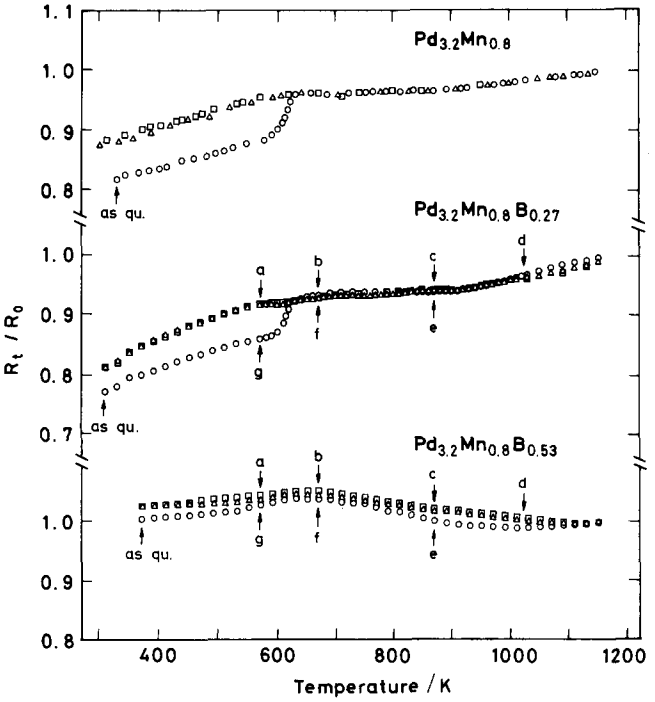

Fig. 6. Electrical resistance ratio R_t/R_0 *vs.* temperature for initially quenched $Pd_{3.2}Mn_{0.8}B_y$ with $y=0$, 0.27 and 0.53 as they are heated (○), subsequently cooled (△) and then reheated (□). The heating and cooling rates were 10 K h^{-1}.

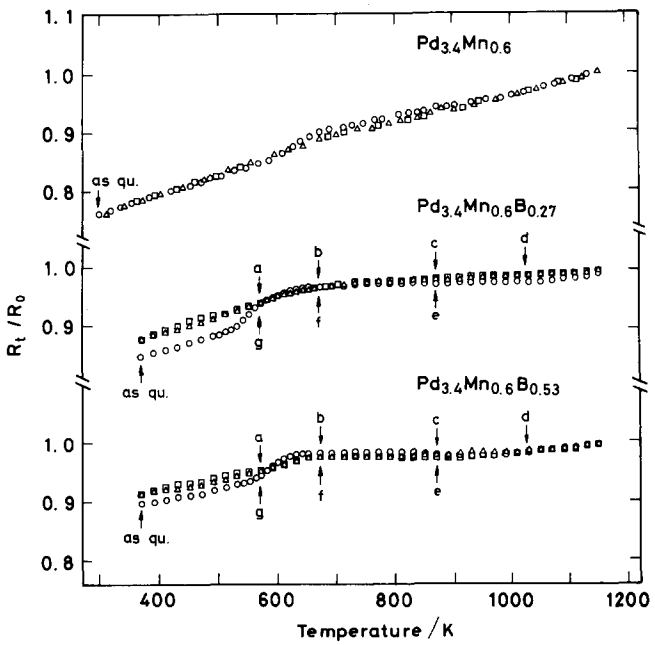

Fig. 7. Electrical resistance ratio R_t/R_0 *vs.* temperature for initially quenched $Pd_{3.4}Mn_{0.6}B_y$ alloys with $y=0$, 0.27 and 0.53 as they are heated (○), subsequently cooled (△) and then reheated (□). The heating and cooling rates were 10 K h^{-1}.

It can be seen from the resistance *vs.* temperature relationships that the changes in resistance of the initially

TABLE 1. Summary of electron diffraction results for $Pd_{3.2}Mn_{0.8}B_y$ and $Pd_{3.4}Mn_{0.6}B_y$ alloys with $y=0$, 0.27 and 0.53 and $Pd_{3.2}Mn_{0.8}M_{0.27}$ alloys with M≡Ag, Cu and Ni during heating and cooling processes: (s), (w) and (d) refer to strong and weak reflections and diffuse scattering respectively in the electron diffraction patterns; "as-quenched indicates that samples were quenched rapidly into ice-water after heating at about 1173 K for 10 min in a stream of argon gas; "annealed" indicates that samples were cooled *in vacuo* to room temperature from about 1153 K at a rate of 10 K h^{-1}

Alloy	Heating process		Cooling process	
	Quenching temperature (K)	Crystal structure	Quenching temperature (K)	Crystal structure
$Pd_{3.2}Mn_{0.8}$	As quenched	Disorder ~$L1_{2-s}$(d)	Annealed	$L1_{2-s}$(d)
$Pd_{3.2}Mn_{0.8}B_{0.27}$	As quenched	$L1_2$(s)+($L1_2$(d)+$L1_{2-s}$(d))	e 873	$L1_2$(s)+($L1_2$(d)+$L1_{2-s}$(d))
	a 573	$L1_2$(s)+($L1_2$(d)+$L1_{2-s}$(d))	f 673	$L1_2$(s)+($L1_2$(d)+$L1_{2-s}$(d))
	b 673	$L1_2$(s)+($L1_2$(d)+$L1_{2-s}$(d))	g 573	$L1_2$(s)+($L1_2$(d)+$L1_{2-s}$(w))
	c 873	$L1_2$(s)+($L1_2$(d)+$L1_{2-s}$(d))	Annealed	$L1_2$(s)+$L1_{2-s}$(w)
	d 1023	$L1_2$(s)+($L1_2$(d)+$L1_{2-s}$(d))		
$Pd_{3.2}Mn_{0.8}B_{0.53}$	As quenched	$L1_2$(s)	e 873	$L1_2$(s)+($L1_2$(d)+$L1_{2-s}$(d))
	a 573	$L1_2$(s)+($L1_2$(d)+$L1_{2-s}$(d))	f 673	$L1_2$(s)+($L1_2$(d)+$L1_{2-s}$(d))
	b 673	$L1_2$(s)+($L1_2$(d)+$L1_{2-s}$(d))	g 573	$L1_2$(s)+($L1_2$(d)+$L1_{2-s}$(d))
	c 873	$L1_2$(s)+$L1_2$(w)	Annealed	$L1_2$(s)+($L1_2$(d)+$L1_{2-s}$(d))
	d 1023	$L1_2$(s)		
$Pd_{3.4}Mn_{0.6}$	As quenched	Disorder	Annealed	$L1_{2-s}$(very d)
$Pd_{3.4}Mn_{0.6}B_{0.27}$	As quenched	$L1_2$(d)+$L1_{2-s}$(d)	e 873	$L1_2$(d)+$L1_{2-s}$(d)
	a 573	$L1_2$(d)+$L1_{2-s}$(d)	f 673	$L1_2$(d)+$L1_{2-s}$(d)
	b 673	$L1_2$(d)+$L1_{2-s}$(d)	g 573	$L1_2$(d)+$L1_{2-s}$(d)
	c 873	$L1_2$(d)+$L1_{2-s}$(d)	Annealed	$L1_2$(d)+$L1_{2-s}$(w)
	d 1023	$L1_2$(d)+$L1_{2-s}$(d)		
$Pd_{3.4}Mn_{0.6}B_{0.53}$	As quenched	$L1_2$(s)+($L1_2$(d)+$L1_{2-s}$(d))	e 873	$L1_2$(s)+$L1_2$(w)
	a 573	$L1_2$(s)+($L1_2$(d)+$L1_{2-s}$(d))	f 673	$L1_2$(s)+($L1_2$(w)+$L1_{2-s}$(d))
	b 673	$L1_2$(s)+($L1_2$(w)+$L1_{2-s}$(d))	g 573	$L1_2$(s)+($L1_2$(w)+$L1_{2-s}$(d))
	c 873	$L1_2$(s)+$L1_2$(w)	Annealed	$L1_2$(s)+($L1_2$(d)+$L1_{2-s}$(d))
	d 1023	$L1_2$(d)+$L1_2$(w)		
$Pd_{3.2}Mn_{0.8}Ag_{0.27}$	As quenched 623	$L1_{2-s}$(d) $L1_{2-s}$(w)	Annealed	$L1_{2-s}$(w)
$Pd_{3.2}Mn_{0.8}Cu_{0.27}$	As quenched 623	$L1_{2-s}$(d) $L1_{2-s}$(w)	Annealed	$L1_{2-s}$(w)
$Pd_{3.2}Mn_{0.8}Ni_{0.27}$	As quenched 623	$L1_{2-s}$(d) $L1_{2-s}$(w)	Annealed	$L1_{2-s}$(w)

quenched samples of boron-containing alloys during heating, subsequent cooling and reheating are similar to the changes in resistance of the boron-free alloys. There is an abrupt increase in resistance of the initially quenched alloys starting at about 593 K for $Pd_{3.2}Mn_{0.8}B_y$ and at about 543 K for $Pd_{3.4}Mn_{0.6}B_y$; thereafter the increase with heating temperature is relatively small and for the highest boron content alloy of $Pd_{3.2}Mn_{0.8}B_y$ with $y=0.53$ the resistance decreases gradually with increasing temperature. The unusual result of the lower resistance of the initially quenched samples compared with the subsequently cooled (annealed) ones arises

from the fact that the former are close to an ordered $L1_2$ structure and/or disordered state rather than the short-range-ordered $L1_{2-s}$ structure. In other words, the subsequently cooled (annealed) samples have more or less the periodic antiphase domain boundaries of $L1_{2-s}$ which would cause electron scattering whereas the quenched alloys do not. The reason for the decrease in resistance of the high boron content alloy of $Pd_{3.2}Mn_{0.8}B_y$ with $y=0.53$ observed during heating in the high temperature region is unknown; the behaviour is reproducible and may be due to the coarsening of the ordered domain of the $L1_2$ structure.

The electron diffraction patterns of the $Pd_{3.2}Mn_{0.8}B_y$ alloy with $y=0.27$, which was quenched from 673 K during heating (point "b", Fig. 6), and for the $Pd_{3.2}Mn_{0.8}B_y$ alloy with $y=0.53$, which was quenched from 873 K during heating (point "c", Fig. 6), are shown in Figs. 8(a)–8(d). It can be seen that even after heating to 673 K, the strong $L1_2$ reflections in $Pd_{3.2}Mn_{0.8}B_y$ with $y=0.27$ remain almost unchanged (Fig. 8(a)). The quenched sample (Fig. 4(a)) also shows $L1_2$ reflections; however, weak and diffuse reflections of superimposed $L1_2$ and $L1_{2-s}$ superlattices are also observed in the as-quenched sample (Fig. 4(b)) which become relatively intense after the 673 K heating (Fig. 8(b)). After heating to 873 K, the initially quenched sample of $Pd_{3.2}Mn_{0.8}B_y$ with $y=0.53$ shows, besides the strong $L1_2$ reflections (Fig. 8(c)) which are observed in some regions of the as-quenched sample, sharp reflection spots due to $L1_2$ in other regions (Fig. 8(d)). As described above, the decrease in resistance during heating corresponds to this stage in which the $L1_2$ reflections appear.

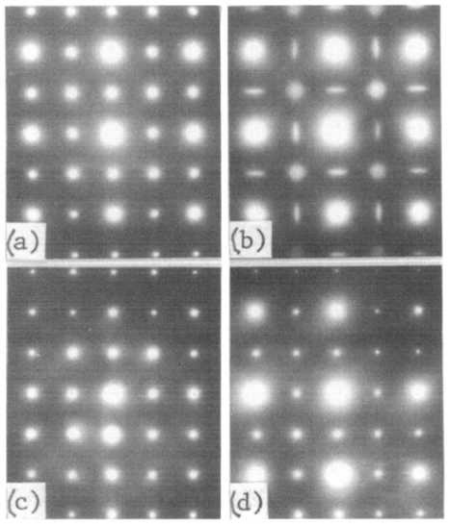

Fig. 8. Electron diffraction patterns with [001] incidence for $Pd_{3.2}Mn_{0.8}B_y$ alloy with $y=0.27$ (a), (b) quenched from 673 K during heating and also for $Pd_{3.2}Mn_{0.8}B_y$ alloy with $y=0.53$ (c), (d) quenched from 873 K during heating.

Figure 9 shows electrical resistance *vs.* temperature relationships for $Pd_{3.2}Mn_{0.8}M_{0.27}$ alloys with M ≡ Ag, Cu and Ni, where M has the same value as B in one of the B-containing alloys but these alloys are substitutional and have been examined for comparison. The shape of the resistance *vs.* temperature relationships of these alloys is almost the same as for the non-additive alloy $Pd_{3.2}Mn_{0.8}$ (Pd–20.0at.%Mn). As can be seen from the results of electron diffraction and transmission electron microscopy observations for these alloys given in Table 1, there is no evidence for the formation of an $L1_2$ structure in the alloys and all the quenched alloys are in an almost disordered state, although the electron diffraction patterns due to $L1_{2-s}$ exhibit very faint reflections, and all the annealed alloys have the short-range-ordered $L1_{2-s}$ structure.

It can be seen from the above results that the formation of the $L1_2$ structure requires the presence of the $L1_{2-s}$ structure and an interstitial boron content greater than a limiting amount of about $y=0.15$. The formation is considered to be initiated at the periodic antiphase domain boundaries of the $L1_{2-s}$ structure by the introduction of a step shift $(\vec{a}_2+\vec{a}_3)/2$ at every two cells along the a_1 axis after attaining a particular stress state as a consequence of the preferential occupation of boron atoms at the octahedral sites consisting of six palladium nearest-neighbour atoms [6], and the

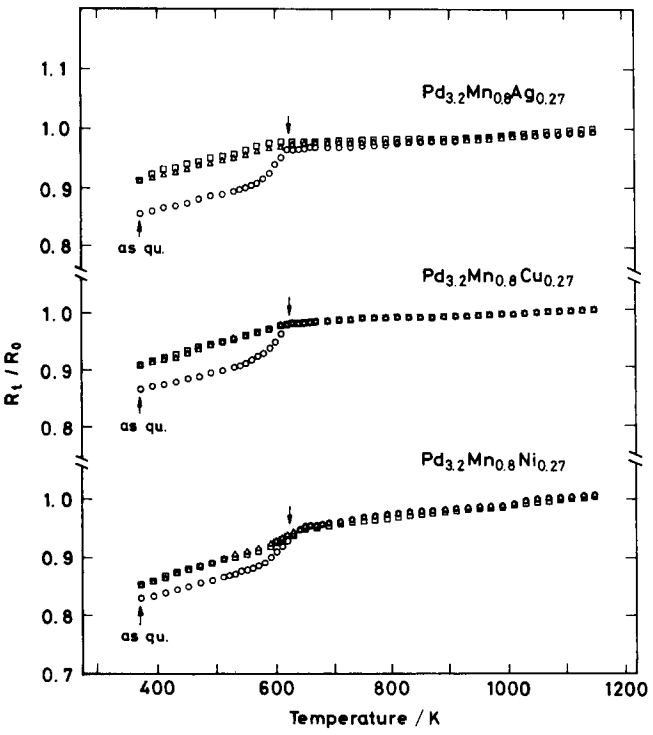

Fig. 9. Electrical resistance ratio R_t/R_0 *vs.* temperature for initially quenched $Pd_{3.2}Mn_{0.8}M_{0.27}$ alloys with M ≡ Ag, Cu and Ni as they are heated (○), subsequently cooled (△) and then reheated (□). The heating and cooling rates were 10 K h^{-1}.

boron atoms of course occupy the octahedral interstices in the α-f.c.c. disordered phase. Boron occupation in the α-f.c.c. disordered phase may precede its occupation in the $L1_{2-s}$ structure. Thus the mechanism for the formation of the $L1_2$ structure in boron-added $Pd_{1+x}Mn_{1-x}B_y$ alloys is similar to that for hydrogen induced ordering to the $L1_2$ structure was observed previously [8, 14].

Acknowledgments

The authors would like to express their gratitude to Tanaka Kikinzoku Kogyo K. K. for the loan of the palladium metal. T. B. F. wishes the thank the National Science Foundation for financial support.

References

1 Y. Sakamoto, K. Takao, Y. Nagaoka, H. Kida and T. B. Flanagan, *J. Alloys Comp.*, in press.
2 D. Watanabe, *Trans. JIM., 3* (1962) 234.
3 H. Sato and R. S. Toth, *Phys. Rev., 139* (1965) A1581.
4 K. Baba, Y. Sakamoto, T. B. Flanagan, T. Kuji and A. P. Craft, *Scr. Metall., 21* (1987) 299.
5 T. B. Flanagan, A. P. Craft, Y. Niki, K. Baba and Y. Sakamoto, *J. Alloys Comp., 184* (1992) 69.
6 P.-J. Ahlzén, Y. Andersson, R. Tellgren, D. Rodic, T. B. Flanagan and Y. Sakamoto, *Z. Phys. Chem. N. F., 163* (1989) 213.
7 C. T. Liu, C. L. White and J. A. Horton, *Acta Metall., 33* (1985) 213.
8 K. Baba, Y. Niki, Y. Sakamoto and T. B. Flanagan, *J. Less-Common Met., 172–174* (1991) 246.
9 K. Baba, Y. Niki, Y. Sakamoto and T. B. Flanagan, *J. Alloys Comp., 179* (1992) 321.
10 R. Burch and F. A. Lewis, *Trans. Faraday Soc., 66* (1970) 727.
11 H. Brodowsky and H.-J. Schaller, *Ber. Bunsenges.. Phys. Chem., 80* (1976) 656.
12 R. A. Alqasmi, H. Brodowsky and H.-J. Schaller, *Z. Metallkd., 73* (1982) 331.
13 Y. Sakamoto, K. Baba and T. B. Flanagan, *Z. Phys. Chem. N. F., 158* (1988) 223.
14 Y. Sakamoto, K. Baba, Y. Niki, Y. Ishibashi and T. B. Flanagan, *J. Alloys Comp., 184* (1992) 57.